12-1-2016

Simulation of the effects of photodecay on long-term litter decay using DayCent

Maosi Chen
Colorado State University

William J. Parton
Colorado State University

E. Carol Adair
University of Vermont

Shinichi Asao
Colorado State University

Melannie D. Hartman
Colorado State University

See next page for additional authors

Recommended Citation

Chen M, Parton WJ, Adair EC, Asao S, Hartman MD, Gao W. Simulation of the effects of photodecay on long-term litter decay using DayCent. Ecosphere. 2016 Dec;7(12):e01631.

esa

ECOSPHERE

Simulation of the effects of photodecay on long-term litter decay using DayCent

Maosi Chen,[1,]† William J. Parton,[2] E. Carol Adair,[3] Shinichi Asao,[1,2] Melannie D. Hartman,[1,2] and Wei Gao[1,4]

[1]*United States Department of Agriculture UV-B Monitoring and Research Program, Natural Resource Ecology Laboratory, Colorado State University, Fort Collins, Colorado 80521 USA*
[2]*Natural Resource Ecology Laboratory, Colorado State University, Fort Collins, Colorado 80523 USA*
[3]*Rubenstein School of Environment and Natural Resources, University of Vermont, Burlington, Vermont 05405 USA*
[4]*Department of Ecosystem Science and Sustainability, Colorado State University, Fort Collins, Colorado 80523 USA*

Citation: Chen, M., W. J. Parton, E. C. Adair, S. Asao, M. D. Hartman, and W. Gao. 2016. Simulation of the effects of photodecay on long-term litter decay using DayCent. Ecosphere 7(12):e01631. 10.1002/ecs2.1631

Abstract. Recent studies have found that solar ultraviolet (UV) radiation significantly shifts the mass loss and nitrogen dynamics of plant litter decomposition in semi-arid and arid ecosystems. In this study, we examined the role of photodegradation in litter decomposition by using the DayCent-UV biogeochemical model. DayCent-UV incorporated the following mechanisms related to UV radiation: (1) direct photolysis, (2) facilitation of microbial decomposition via production of labile materials, and (3) microbial inhibition effects. We also allowed maximum photodecay rate of the structural litter pool to vary with litter's initial lignin fraction in the model. We calibrated DayCent-UV with observed ecosystem variables (e.g., volumetric soil water content, live biomass, actual evapotranspiration, and net ecosystem exchange), and validated the optimized model with Long-Term Intersite Decomposition Experiment (LIDET) observations of remaining carbon and nitrogen at three semi-arid sites in Western United States. DayCent-UV better simulated the observed linear carbon loss patterns and the persistent net nitrogen mineralization in the 10-year LIDET experiment at the three sites than the model without UV decomposition. In the DayCent-UV equilibrium model runs, UV decomposition increased aboveground and belowground plant production, surface net nitrogen mineralization, and surface litter nitrogen pool, but decreased surface litter carbon, soil net nitrogen mineralization, and mineral soil carbon and nitrogen. In addition, UV decomposition had minimal impacts on trace gas emissions and biotic decomposition rates. The model results suggest that the most important ecological impact of photodecay of surface litter in dry grasslands is to increase N mineralization from the surface litter (25%), and decay rates of the surface litter (15%) and decrease the organic soil carbon and nitrogen (5%).

Key words: arid and semi-arid grassland ecosystems; DayCent-UV model; Long-Term Intersite Decomposition Experiment; photodegradation; shortgrass; solar ultraviolet radiation; surface litter decomposition.

Received 25 October 2016; accepted 31 October 2016. Corresponding Editor: Michael F. Allen.

† **E-mail:** maosi.chen@colostate.edu

Introduction

The carbon (C) and nitrogen (N) balance between the atmosphere and terrestrial biosphere is driven by the two fundamental processes of production and decomposition (Olson 1963, Moorhead et al. 1999). The physical and biological mechanisms behind production such as photosynthesis and photosynthate allocation are relatively well understood (Cramer et al. 1999). It is well known that solar radiation, precipitation, temperature, and N availability are key controlling parameters on net primary production (Cramer et al. 1999, Nemani et al. 2003).

However, the mechanisms behind litter decomposition, particularly in arid systems, are not fully clear (Dirks et al. 2010, Austin 2011, King et al. 2012). Decomposition is the primary controller on the cycling of C and N among plants, soil, and the atmosphere (Melillo et al. 1982, Moorhead et al. 1999). Decomposition releases N for plant production and microbial activity (Parton et al. 2007) and releases CO_2 into atmosphere (~53–57 Pg/yr [C], Harmon et al. 2011) at much higher rate than fossil fuel carbon emission (~7.8 Pg/yr [C], Ciais et al. 2013). Thus, small changes in litter and soil decomposition rate could result in large variation in atmospheric CO_2 concentration (Adair et al. 2008, Bond-Lamberty and Thomson 2010).

Plant litter decomposition influences the formation of soil organic matter (SOM), the mineralization of organic nutrients, and the carbon balance in terrestrial ecosystems (Moorhead et al. 1999). In mesic ecosystems, the rate of litter decomposition is determined by litter chemistry especially lignin content (phenolics) and lignin to nutrient ratios (Meentemeyer 1978, Melillo et al. 1982). Usually, litter with low carbon to nitrogen (C/N) ratio and low lignin content decomposes fast, and roots, which have more recalcitrant compounds (e.g., lignin), decompose slowly (Pérez-Harguindeguy et al. 2000, Zhao et al. 2014). This pattern is predicted by traditional decomposition models that focus on the roles of microbes on decomposition. These models mainly use climate variables (i.e., precipitation and temperature) and litter quality variables (C/N, the lignin to nitrogen ratio [lignin/N]) to simulate litter mass loss patterns (Meentemeyer 1978, Parton et al. 1987).

In semi-arid/xeric ecosystems, however, litter decomposition is faster than predicted by models which are only driven by climate and litter chemistry (Whitford et al. 1981, Moorhead and Callaghan 1994, Moorhead et al. 1999, Parton et al. 2007, Foereid et al. 2011). Furthermore, in arid systems a portion of decomposing surface litter does not immobilize nitrogen and the decomposition rate is often unrelated to initial N contents (Parton et al. 2007, Gallo et al. 2009). These patterns suggest that abiotic processes rather than microbial activity may be an important driver of decomposition in arid ecosystems (Parton et al. 2007). Indeed, field experiments show that abiotic photodegradation has significant impacts on litter decay (e.g., mass loss rate, CO_2 emissions, and litter chemistry) in arid deserts (Day et al. 2007), in semi-arid grasslands and shrublands (Austin and Vivanco 2006, Rutledge et al. 2010), and in high-latitude forest ecosystems (Moody et al. 2001). Day et al. (2007) concluded that ultraviolet-B (UV-B) is responsible for 14–22% of total litter mass loss in arid and hot sites. Foereid et al. (2011) found that up to 14% of net primary productivity (NPP) is photodegradable in dry and high radiation ecosystems. Gallo et al. (2006) concluded that UV radiation alone, or in combination with microbial activity, is as effective at decomposing litter in arid ecosystems as microbial activity alone in mesic ecosystems.

The mechanistic detail of photodegradation remains uncertain (King et al. 2012). It is reported that UV radiation may directly photolyze a molecule through fragmentation, intramolecular rearrangement, or electron transfer (King et al. 2012, Lee et al. 2012). UV radiation may also indirectly photolyze a non-light-absorbing molecule by promoting the production of reactive intermediates (e.g., singlet oxygen and hydroxyl radical) created from some molecules (often triplet oxygen) receiving energy transferred from radiation absorbing photosensitizers (George et al. 2005, Messenger et al. 2009, Cory et al. 2010, Feng et al. 2011, King et al. 2012). However, uncertainties exist surrounding the specific carbon compounds that are affected by photodegradation, with some evidence for higher loss rates from either cellulosic or lignin pools (Rozema et al. 1997, Austin and Ballaré 2010, King et al. 2012, Song et al. 2013, Austin et al. 2016). UV radiation may also have important indirect impacts on decomposition: (1) facilitating microbial decomposition via the generation of labile material from photodegradation (Gallo et al. 2006, Henry et al. 2008, Andrady et al. 2011, Liu et al. 2014, Almagro et al. 2015, Baker and Allison 2015, Austin et al. 2016) or facilitating leaching by breaking down cell walls and releasing fats and lipids (Vähätalo et al. 1998, Day et al. 2007, Lin and King 2014); and (2) decelerating decomposition by reducing microbial populations and respiration (Gehrke et al. 1995, Zepp et al. 1998, Hughes et al. 2003), altering microbial community composition by selecting species that can tolerate extreme climate conditions, repair DNA efficiently, or synthesize photoprotective pigments (Gehrke

et al. 1995, Moody et al. 2001, Pancotto et al. 2003, 2005), reducing N immobilization (Lin et al. 2015*b*, Wang et al. 2015) and reducing extracellular enzyme activity (Gallo et al. 2009).

Several studies have investigated the effective wavelength range of solar radiation for photodegradation and found that both UV-B (280–320 nm) and the rest of the solar spectra (Austin and Vivanco 2006), or both UV radiation (280–400 nm) and shortwave visible radiation (400–500 nm or 400–550 nm; Austin and Ballaré 2010, Brandt et al. 2009) have significant contribution to photodegradation. Although UV-B radiation has higher per photon energy than UV-A radiation, the abundance of UV-B reaching the ground is much smaller than that of UV-A due to the preferential absorption of shorter wavelength UV by the stratospheric ozone. As a result, the overall role of UV-A radiation on photodegradation is comparable to that of UV-B radiation (King et al. 2012). Therefore, more recent studies have been using the UV radiation (280–400 nm) instead of UV-B radiation alone as the wavelength range for photodegradation research (Baker and Allison 2015, Lin et al. 2015*a*, *b*, Wang et al. 2015).

In this study, we examined the role of photodegradation in litter decomposition using DayCent-UV which is the extension of the DayCent biogeochemical model with a photodecay submodel. The widely tested hypotheses supporting flows related to UV radiation induced direct photolysis, facilitation effects, and microbial inhibition effects were incorporated in DayCent-UV. In this study, DayCent-UV was used to simulate the semi-arid shortgrass steppe ecosystem at three western US sites. First, the model parameters were adjusted to match the observations of soil water content, plant growth pattern, actual evapotranspiration (AET), and net ecosystem exchange (NEE) at a calibration site. Second, the model was configured to simulate the LIDET decomposition experiment from the 1990s for six common litter types at the three arid sites. A subset of the photodegradation-related parameters were optimized for each species individually and across species using a global optimization algorithm that combines scatter search and non-linear trust region optimization algorithms. Third, DayCent-UV with optimized parameters was validated at the other two sites. Finally, the long-term (i.e., 90 yr) impacts of photodegradation on ecosystem processes such as plant productivity, C and N pools, N mineralization, and trace gas emissions were explored.

Methods

Sites and data

CPER.—DayCent-UV was calibrated with the measurements made at the United States Department of Agriculture—Agricultural Research Services (USDA-ARS) Central Plains Experimental Range (CPER) site (latitude: 40.816° N, longitude: 104.749° W, elevation: 1646 m). CPER site is a Long Term Ecological Research (LTER) site located at the western edge of the Central Great Plains in Colorado. CPER has mean annual precipitation of 434 mm, mean annual air temperature of 9.31°C, and mean annual total solar radiation of 462.63 W/m^2 between 1990 and 1999. Much of the precipitation occurs from April to June (43%; Parton et al. 2012). The vegetation at CPER site is dominated by *Bouteloua gracilis* (C4 grass) with a mixture of other C4 and C3 grasses, shrubs, forbs, and cacti (Parton et al. 2012). Long-term mean annual aboveground net primary productivity (ANPP) is 97 g/m^2 (dry mass; Heisler-White et al. 2008), and mean leaf area index is low (<1, Brandt et al. 2007). The pastures were subjected to zero, moderate, and heavy grazing treatments with 0%, 40%, and 65% of annual forage production removed, respectively (Parton et al. 2012).

Four types of measurements were made and averaged at daily time resolution at CPER site between 2001 and 2003. The measurements were NEE, AET, volumetric soil water content (VSWC), and aboveground live biomass. Both NEE and AET were measured or estimated using the Bowen ratio energy balance (BREB) system (Model 023/CO2 Bowen ratio System, Campbell Scientific Inc., Logan, UT, USA; Irmak et al. 2008, Parton et al. 2012). Volumetric soil water content for top 0–15 cm soil was measured using water content reflectometers (Model CS615, Campbell Scientific; Parton et al. 2012). Aboveground live biomass during growing season (i.e., late April to end of September) was measured in nine randomly selected one-meter squared quadrants around the BREB towers (Parton et al. 2012).

LIDET.—Long-Term Intersite Decomposition Experiment (LIDET, Harmon 2013) is a 10-year (1990–1999) study of litter decomposition and

Table 1. Climatic characteristic and ecosystem type for the three selected LIDET sites (Gholz et al. 2000, Adair et al. 2008).

Site	Lat. (°)	Lon. (°)	Elev. (m)	MAT (°C)	MAP (mm)	SR W/m^2	AET (mm)	DEFAC	CDI_{LT}	Ecosystem type
Central Plains Experimental Range (CPER)	40.82° N	104.77° W	1650	8.60	440	462.6	430	0.19	0.243	Dry grassland
Sevilleta National Wildlife Refuge (SEV)	34.33° N	106.67° W	1572	13.17	255	520.6	252	0.10	0.136	Shrubland/desert
Jornada Experimental Range (JRN)	32.50° N	106.75° W	1410	17.15	298	526.1	292	0.13	0.216	Shrubland/desert

Notes: All climatic variables were averages of the 10-year LIDET study period (1990–1999). CDI_{LT} is the Lloyd and Taylor (1994) climate decomposition index. DEFAC is a complex climatic factor related to decomposition in the CENTURY model. The terms "Lat.," "Lon.," and "Elev." are the abbreviation of latitude, longitude, and elevation. The terms "MAT," "MAP," and "SR" stand for mean annual temperature, precipitation, and solar radiation. The term "AET" stands for actual evapotranspiration.

nutrient dynamics in response to substrate quality and macroclimate (Gholz et al. 2000, Parton et al. 2007). LIDET data were provided by the HJ Andrews Experimental Forest research program, funded by the National Science Foundation's Long-Term Ecological Research Program (DEB 08-23380), US Forest Service Pacific Northwest Research Station, and Oregon State University. The experiment was conducted at 28 sites in North and Central America that reflected a wide variety of natural ecosystems and climates (Long-Term Intersite Decomposition Experiment Team 1995, Gholz et al. 2000). All 28 sites had nine common litters, fine roots from three species and leaf from six species covering a wide range of initial litter chemistry, and one "wildcard" litter type at each site (Long-Term Intersite Decomposition Experiment Team 1995, Adair et al. 2008). Although the litterbag method used by LIDET has known limitations, including the relatively low sampling intervals (i.e., 1 yr for LIDET); light attenuation by cumulated litter and soil on litterbags; higher and more stable moisture inside litterbag both at dry and wet sites; and potential exclusion of macrofauna by the mesh of litterbag (Hutchinson et al. 1990, Virzo De Santo et al. 1993, Kurz-Besson et al. 2005), it remains the best available method for investigating long-term decomposition patterns (Adair et al. 2008).

The three LIDET sites used in this study were Central Plains Experimental Range in Colorado (CPER) and Sevilleta (SEV) and Jornada (JRN) in New Mexico. The sites are dry and receive high UV radiation, and surface litter decomposition rates at these sites were not well explained by macroclimate and litter quality only (Parton et al. 2007, Adair et al. 2008). The LIDET CPER site was the same location as the USDA-ARS CPER site that was used to calibrate the DayCent-UV SOM decomposition submodel. The other two sites, SEV and JRN, were used to test the performance of the calibrated DayCent-UV model. The annual aboveground net primary production for SEV and JRN sites was 83 and 130 g/m^2 (dry mass; Peters et al. 2013), respectively. The climatic characteristic and ecosystem type for the three selected LIDET sites are summarized in Table 1.

The six common leaf litter species (*Acer saccharum* [ACSA], *Drypetes Glauca* [DRGL], *Pinus resinosa* [QUPR], *Quercus prinus* [THPL], *Thuja plicata* [THPL], and *Triticum aestivum* [TRAE]) were used to calibrate and validate the model performance in this study. The initial values of litter quality indices for these six species are listed in Table 2 (extracted from Adair et al. 2008).

It is noted that other than LIDET, there are other long-term litter decomposition data set available such as Decomposition Study (DECO; Berg et al. 1993) in Europe and Eastern United States and Canadian Intersite Decomposition Experiment Team (CIDET; Trofymow et al. 1995) in Canada. Since we have more prior knowledge of the soil, plant, and management strategies at the collocated CPER site and the other two LIDET sites have a similar environment, we chose LIDET as the data source for this study.

UV radiation parameterization

The solar UV (280–400 nm) radiation is the sum of the solar UV-B (280–320 nm) and UV-A (320–400 nm) radiation. Both the UV-B and UV-

Table 2. Initial values of litter quality indices for the six common leaf litter species in the LIDET experiment (extracted from Adair et al. 2008).

Species	Litter type	Abbreviation	Water-soluble extractives† (%)	Cellulose (%)	Lignin (%)	C/N
Acer saccharum (Sugar Maple)	Broadleaf	ACSA	47.68	27.33	15.87	61.83
Drypetes Glauca (Drypetes)	Broadleaf	DRGL	40.23	39.82	10.91	24.25
Pinus resinosa (Red Pine)	Conifer	PIRE	20.60	44.58	19.18	92.72
Quercus prinus (Chestnut Oak)	Broadleaf	QUPR	27.22	39.38	23.51	50.55
Thuja plicata (Western Redcedar)	Conifer	THPL	22.31	35.92	26.67	83.12
Triticum aestivum (Wheat)	Graminoid	TRAE	6.72	73.15	16.21	133.32

† Water-soluble extractives mean labile C contents in litter.

A radiations reaching the Earth's surface depend on the site location, their top of the atmosphere counterparts (constant if earth–sun distance is normalized), clouds, total column ozone, aerosols, surface albedo, and atmospheric profiles. In addition, the solar total radiation (280–2800 nm, TSR) at ground also depends on the abundance of column water vapor and trace gases. When all these data are available, it is possible to directly simulate both UV and TSR with the assistance of a radiative transfer model such as MODTRAN (http://modtran5.com/, Berk et al. 2006, Anderson et al. 2009). But for most sites, it may be difficult to prepare all of these data. Therefore, less accurate but simple approaches were developed to simulate daily TSR from daily temperature and site location (Bristow and Campbell 1984, Thornton and Running 1999) and to simulate daily UV from daily TSR with linear regression (Escobedo et al. 2010). In this study, the MODTRAN (v5.3) model was set up to simulate the daily TSR and daily UV for a whole year at three sites with the site-specific locations and total column ozone, the standard atmosphere profile, aerosol loading, and surface albedo, and a wide variety of cloud optical thickness (i.e., 0.0–7.8). The regressions showed that the ratios between daily UV and daily TSR are around 6.02–6.08% (R^2s around 0.99) at CPER, SEV, and JRN sites. It should be noted that since standard atmospheric parameters are used, these ratios only represent the typical or average cases at these sites and may be slightly different in real cases.

DayCent model

Original DayCent.—DayCent (Parton et al. 1998, Del Grosso et al. 2001, 2011) is a daily time step biogeochemical model that simulates exchanges of water, carbon and nutrients (nitrogen [N], phosphorus [P], and sulfur [S]) among the atmosphere, soil and plants as well as plant phenology and management events (e.g., fire, grazing, cultivation, and organic matter addition). The DayCent model inputs (Del Grosso et al. 2011) include daily weather data (e.g., minimum and maximum temperatures, precipitation, and solar radiation), soil properties by layer (e.g., bulk density, field capacity, wilting point, texture, root fraction, and saturated hydraulic conductivity), site latitude and longitude and weather, crop cultivar parameters (e.g., temperature and water stress functions, respiration, growth, and death rates, and relative C allocation among plant parts), and management information. The four primary submodels are plant production, soil carbon and nutrient dynamics, soil water and temperature dynamics, and trace gas fluxes (Del Grosso et al. 2001, 2011). The DayCent model has been used extensively to simulate ecosystem dynamics for agricultural ecosystems (Del Grosso et al. 2005, Stehfest et al. 2007), grasslands and savannas (Parton et al. 2011, 2012), and forest systems (Savage et al. 2013) and has been tested extensively against observed data sets (e.g., nitrous oxide emission, crop yield, and soil C and N [Del Grosso et al. 2008]).

Plant production (NPP) is a function of genetic potential, solar radiation, phenology, water and temperature conditions, and nutrients availability (Del Grosso et al. 2008). The allocation of NPP among plant components (e.g., shoots and mature and juvenile roots for crop/grass) is controlled by vegetation type, phenology, and water/nutrient stress (Del Grosso et al. 2008). The death rate of plant parts is controlled by soil water, temperature, season, and plant-specific senescence parameters (Del Grosso et al. 2011).

The SOM submodel simulates carbon and nutrient flows for the surface and SOM pools (structural and metabolic litter, and active, slow, and passive SOM; Parton et al. 1987, 1988). Major controls on these flows include litter lignin content and C/N ratios, temperature/water decomposition factors, and soil texture (Del Grosso et al. 2001). The nutrient pool is supplied by decomposition of SOM, N fixation, and external nutrient addition such as fertilization and atmospheric N deposition (Del Grosso et al. 2001). The C and N fluxes between litter and SOM pools in DayCent are summarized in Appendix S1.

The land surface submodel of DayCent simulates soil temperature with depths as well as water flow through the plant canopy, litter, and soil profile (Parton et al. 1998, Del Grosso et al. 2011). The N-gas submodel of DayCent simulates soil N_2O, NO_x, and N_2 gas emissions from nitrification and denitrification (Del Grosso et al. 2000, 2011, Parton et al. 2001).

DayCent-Photosyn.—DayCent-Photosyn (Straube 2011) incorporates the SIPNET (Simple Photosynthesis and Evapo-Transpiration) model (Braswell et al. 2005), a simplified Farquhar plant photosynthesis and respiration model (Savage et al. 2013). Compared to earlier versions of DayCent, DayCent-Photosyn adds the capability of simulating the gross primary production and includes a carbon storage pool that is fueled by photosynthesis and supports the maintenance respiration, actual NPP, and growth respiration. The calculation of actual NPP and growth respiration in DayCent-Photosyn follows the strategy used by DayCent, but the demanded C of the two processes is withdrawn from the carbon storage pool.

DayCent-UV.—Traditional decomposition models fail to accurately predict the atypical linear pattern of aboveground litter mass loss in the arid environment, suggesting that photodegradation should be considered in a decomposition model (Parton et al. 2007). Other studies have suggested the following direct and indirect effects of solar UV radiation on surface plant litter decomposition:

(1) UV photodegradation increases litter biodegradability by increasing labile C supply (Wang et al. 2015) and produces C-based gases (Brandt et al. 2009, Lee et al. 2012). The most efficient wavelength range for photodegradation (i.e., UV and shortwave visible spectra) has strong correlation with the absorption spectrum of lignin but not cellulose (Austin and Ballaré 2010). Some studies observed significant lignin loss when litter was exposed to UV radiation and concluded that lignin is preferentially degraded by photodegradation (Day et al. 2007, Henry et al. 2008, Austin and Ballaré 2010, Liu et al. 2014). Wang et al. (2015), however, did not observe lignin loss with UV exposure but without microbial decomposition and suggested that the significant decrease in lignin content when litter was exposed to UV radiation was a combined effect of abiotic and biotic decomposition. One reasonable explanation is that the UV radiation absorbed by lignin may change its chemical structure and increase its accessibility to microbial enzymes (Wang et al. 2015, Austin et al. 2016).

(2) UV radiation decelerates decomposition by reducing microbial population and respiration (Gehrke et al. 1995, Zepp et al. 1998, Hughes et al. 2003, Pancotto et al. 2003). The reason of the reduction is that the decomposers, microbes, can be directly and indirectly damaged by UV radiation via the absorption of photons by DNA (Caldwell et al. 1998, Fernández Zenoff et al. 2006). UV-A light indirectly damages DNA by producing reactive oxygen intermediates which can cause strand breaks and DNA–protein cross-links (Kielbassa et al. 1997, Kurbanyan et al. 2003, Fernández Zenoff et al. 2006). The absorbed UV-B radiation can also cause direct DNA damage by dimerization of pyrimidine with two major photoproducts: cyclobutane pyrimidine dimers and pyrimidine (6-4) pyrimidone photoproducts (Mitchell and Karentz 1993, Caldwell et al. 1998).

Based on these mechanisms, three kinds of modifications were incorporated into DayCent-UV: (1) adding photodegradation fluxes from the cellulosic (intermediate) pool to increase abiotic mass loss of litter (Similar to the traditional microbial decomposition, the litter's lignin content controls the maximum photodegradation rate [maxphoto]); (2) allowing a fraction of the photodegradation flux to enter the labile pool to facilitate litter decomposition; and (3) slowing the labile pool's decomposition and increasing the turnover rates between the surface active pool and slow pool to simulate the inhibitive effect of UV radiation on microbial activity.

More specifically, DayCent-UV includes the following modifications (Fig. 1): (1) a direct C

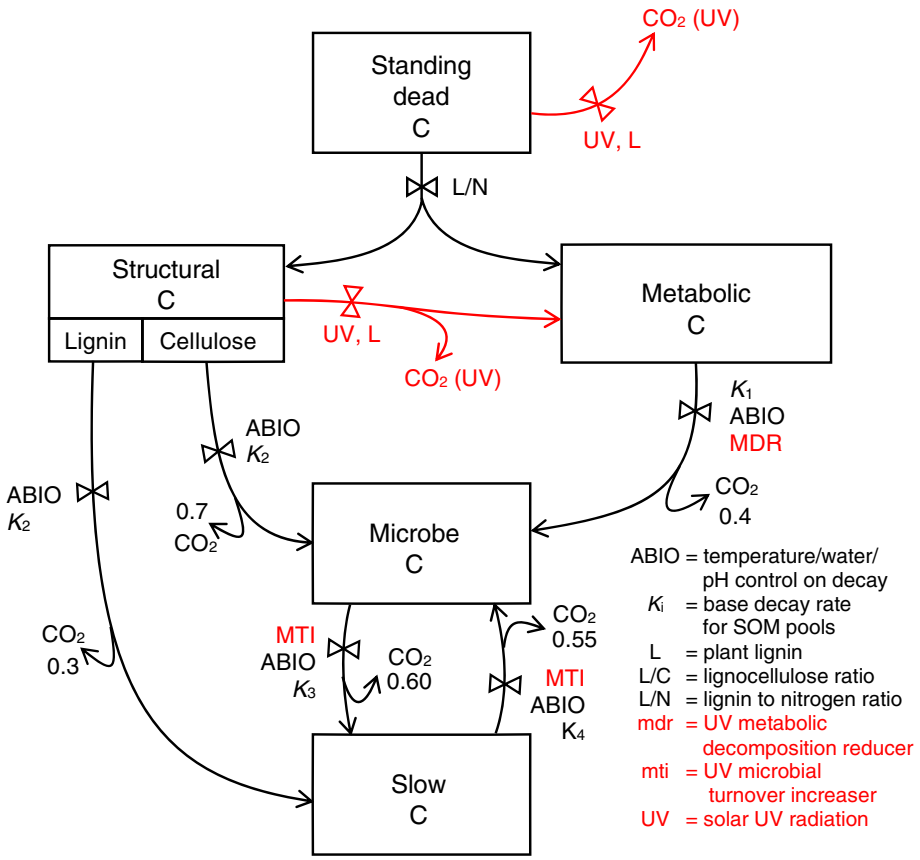

Fig. 1. Surface carbon pools and flows represented in DayCent-UV. The pools are shown in rectangular boxes; the flows between the pools are shown by arrowed lines; and the CO_2 flux associated with the flows are shown by arrowed curves. The numbers near the end of curve arrows are the fraction of C flow that is lost to the atmosphere as CO_2 flux. The abiotic factors that control the decomposition process include UV (soil surface solar UV radiation), soil temperature, soil moisture, and pH. The term mdr is the metabolic decomposition reducer, which is negatively related to the ground level solar UV radiation. The term mti is the microbial turnover rate increaser, which is positively related to the ground level solar UV radiation. Microbe C is another name for the active C pool.

loss as CO_2 due to photodecomposition of standing dead material, (2) a direct C loss as CO_2 during the breakdown of large structural compounds in surface litter, (3) a transfer of C and N from photodegraded surface structural litter to surface metabolic litter; (4) a reduction of the decomposition rate of the surface metabolic by higher UV radiation via the metabolic decomposition reducer (mdr); and (5) an enhancement of the turnover rates between the surface active ("MICROBE C" in Fig. 1) and the surface slow ("SLOW C" in Fig. 1) by higher UV radiation via the microbial turnover increaser (mti). The added flows (1) and (2) increase abiotic mass loss of litter due to photodegradation. The added flow (3) facilitates litter decomposition by providing more labile materials. The modified flows (4) and (5) simulate the effects of UV radiation on microbial activity. The equations which describe the flows of C and N in DayCent-UV (Appendix S2) and the estimation of daily solar radiation from daily minimum and maximum temperatures (Appendix S3) are presented in the online material. The impact of lignin content on photodecay rate has been implemented in DayCent-UV (Appendix S2).

Simulation of LIDET experiment in DayCent-UV

We calibrated DayCent-UV to simulate the LIDET experiment for six leaf litter types at three sites (i.e., CPER, SEV, and JRN). DayCent-UV has four distinct pools to represent surface organic matter: structural and metabolic pools that represent plant litter, and active (microbe) and slow pools that represent decomposing organic matter (Fig. 1). To configure the model for these experiments, the surface pool was cleared at the beginning of the simulation with a fire event, and 100 g of organic matter was added to surface structural and metabolic pools with the C/N ratio and lignin fraction matching the leaf litter for the LIDET experiment (Adair et al. 2008). To simulate the conditions of LIDET litter bags, no new litter from standing dead and dead fine roots was allowed to enter any surface pools during the 10-year period. Similarly, the surface pools were not allowed to mix with SOM pools. The quantities of organic C and N in the four surface organic matter pools were tracked during the simulation as remaining C and N fractions of the initial litter.

Model parameterization

Use of generalized parameters will likely lead to poor model performance and tuning input variables of the model is needed to better represent site-specific conditions (Del Grosso et al. 2011). Following the suggested order of model calibration (Del Grosso et al. 2011) and the available observed data, the input parameters related to the soil water content, plant growth pattern, evapotranspiration, and photosynthesis were adjusted. Plant production, photosynthesis, and soil water submodels were calibrated with observed daily net ecosystem carbon exchange, soil water (0–20 cm depth) and AET rates, and seasonal changes in live biomass from 2001 to 2003 (Parton et al. 2012). The photodecay module in DayCent-UV was calibrated with LIDET litter decay observations from the Colorado site. LIDET observations from two sites in New Mexico (SEV and JRN) were used as an independent validation of the ability of DayCent-UV to simulate mass loss and nitrogen release from surface litter.

Observed soil texture and soil water data at CPER site (Parton et al. 2012) were used to estimate the field capacity, wilting point, and minimum water content for the different soil layers. The soil physical properties for each soil layer, such as bulk density, saturated hydraulic conductivity, snow melt parameter, and live root fractions, were also adjusted. The snow equivalent precipitation amount was adjusted (increased by 75%) in the winter to early spring period based on observed daily rain gauge and lysimeter data showing that the rain gauge substantially underestimated water inputs for snow events. The scaling factor for potential evapotranspiration and the damping factor (a multiplier that controls unsaturated water flux between adjacent soil layers) were reduced, and the duration of each rain event was increased in order to better represent the observed daily soil water data and AET data (2001–2003). Daily maximum and minimum air temperatures and precipitation data (1969–2010) at CPER site were obtained from multiple sources (Parton et al. 2012, Parton 2013, National Centers for Environmental Information, NOAA 2015, National Water and Climate Center, NRCS, USDA 2015, Rangeland Resources Research Unit, ARS 2015) with the highest quality possible. We used the soil physical properties (field capacity, wilting point, bulk density, etc.) at CPER site and the observed site-specific solar and weather data for the SEV and JRN sites' computer runs. The solar radiation and maximum and minimum air temperatures and precipitation data of the SEV and JRN sites were from multiple sources (Jornada Basin LTER 2012, Moore 2014, National Centers for Environmental Information, NOAA 2015, Physical Sciences Division, ESRL, NOAA 2015).

The main data sets we used to parameterize the plant growth submodel include the observed seasonal change in live leaf biomass (2001–2003), daily observed daytime and nighttime NEE data (2001–2003), and observed historical plant production data at CPER site (Lauenroth 2013). The live biomass data and NEE data were used to parameterize the plant phenological controls on plant growth and maximum photosynthesis rate (e.g., reduced growth and photosynthesis rates at the end of the growing season). The live biomass data were used to parameterize the impact of soil water stress on plant growth. The 30-year observed plant production data were used to adjust temperature growth curves and atmospheric N deposition inputs. The net effect of the

model parameter changes was to increase the impact of drought stress on plant growth, reduce the impact of nitrogen stress on plant growth, and replicate the observed seasonal live biomass patterns showing highest live biomass in June and a sharp decrease in live biomass in July. We also made a change to the equations which simulate enhanced SOM decay rates following rainfall events during the growing season based on the observed NEE data sets.

Because there is no observed solar radiation data for the equilibrium runs and daily solar radiation and temperatures are correlated, the model uses daily temperature data to estimate the daily total solar radiation and applies a site-specific monthly cloud and aerosol adjustment coefficient to get the total solar radiation estimate. The model used observed solar radiation data sets (Physical Sciences Division, ESRL, NOAA 2015) to calibrate the 12 solar radiation monthly adjustment coefficients. The same calibration process was used for CPER, JRN, and SEV sites.

The LIDET mass and nitrogen remaining data from the six different surface litter decay results from CPER site were used to parameterize UV litter decay parameters. We used a model optimization program to calculate the optimal values of the parameters. It is a global optimization method that combines the scatter search framework (Laguna and Martí 2003) and gradient-based nonlinear trust region optimizer (Conn et al. 2000, Ugray et al. 2007). We defined a non-dimensionalized objective function for the optimization method to evaluate the performance of DayCent-UV parameters on fitting multiple types of observational variables (i.e., surface remaining C and N fractions). The same numerical optimization procedure was used to determine the parameters for the plant production submodel. The detailed design of the optimization method is found in the online material (Appendix S6). The optimal value for the model parameters were used if the optimal values made biological sense. If optimal values did not make biological sense, we manually adjusted some of the optimal parameter values based on general biological knowledge. In general, however, the optimization process was quite useful for identifying the critical parameters which impact the fit to the observed data sets. The values for the model input parameters changes made during model optimization process are found in online material (Appendices S4 and S5) and on the Century website (http://www.nrel.colostate.edu/projects/daycent/). The Century website contains all of the information needed to run DayCent-UV for CPER, JRN, and SEV sties.

Results

Model performance on ecosystem variables

The details of DayCent-UV performance on ecosystem variables are described in online material (Appendix S7). Generally, the modeled and observed VSWC in the first 0 to 20 cm soil layer, aboveground live biomass, and AET agreed well (with R^2 ranged from 0.44 to 0.50) in the 3-year period (i.e., 2001–2003). It is noted that the modeled and observed NEE had a less agreement (R^2 = 0.2301) in the same time period.

UV model verification and validation

The performance of the DayCent-UV model was examined by comparing model results to the observed C and N fraction remaining vs. time for the six common litter species in the 10-year LIDET experiment (i.e., 1990–1999) at CPER calibration site (Fig. 2). A scatterplot of the DayCent-UV simulation vs. data as a function of plant species is shown in Fig. 3. The observed time series of remaining C fraction showed that some of the species followed a more exponential pattern of C loss (ACSA and DRGL), while the other species displayed a more linear pattern for C release vs. time. There were considerable species differences in the C loss rates with DRGL and TRAE losing the most C, although species DRGL and TRAE did not have common traits such as the initial C/N ratio and lignin content. There was also a general pattern of less C loss with increasing lignin content of the litter (THPL had the highest lignin content and the lowest C loss). The comparison of the observed vs. simulated C remaining vs. time suggested that DayCent-UV consistently overestimated the decomposition rate in the early stage (i.e., first 3 years). The scatterplot of observed and simulated C remaining for all of the species (Fig. 3A) showed that the model tended to underestimate C remaining when observed C remaining was greater than 0.5 and overestimate C remaining when observed C remaining was less than 0.3. The model performance of DayCent-UV, which allows maxphoto (the maximum photodecay rate)

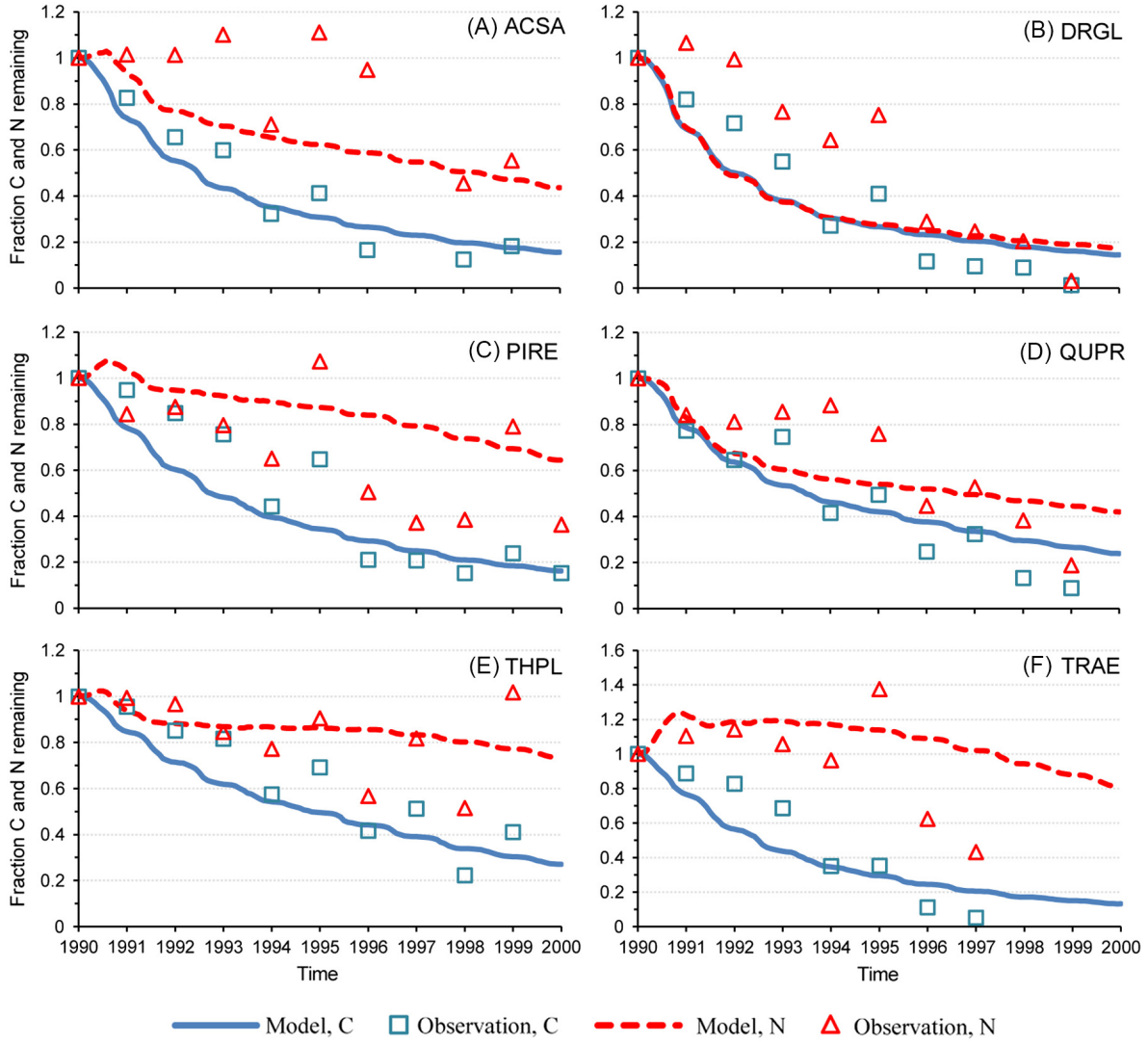

Fig. 2. The time series of remaining C and N (fraction) in litter bags for six litter species (i.e., ACSA, DRGL, PIRE, QUPR, THPL, and TRAE) from DayCent-UV (solid lines for C and dashed lines for N) and from the annual observation of LIDET experiment (squares for C and triangles for N) at Colorado (CPER) site.

to linearly vary with litter's initial lignin content (Appendix S2), varied by litter species. The model results showed that DayCent-UV had the best performance on species THPL (0.13 [RMSE for C], 0.17 [RMSE for N]) followed by ACSA (0.10, 0.27), QUPR (0.12, 0.19), TRAE (0.16, 0.32), PIRE (0.16, 0.26), and DRGL (0.14, 0.32). There was no obvious correlation between the model performance and the initial C/N ratios and lignin content of litter.

The observed N data had larger differences among the litter species and large unexplained changes in the observed N remaining vs. time (e.g., N remaining for PIRE goes from 0.65 in 1994 to 1.1 in 1995 and then decreases to 0.5 in 1996; Fig. 2). The observed fraction of N remaining showed a general pattern of decreased N with increasing time for most species; however, for TRAE and PIRE, it increased to greater than 1.0 (up to 1.4) at 5 years after the beginning of the experiment. DayCent-UV simulated the observed pattern of increased N losses with time. The overall RMSE values for the model vs. data comparison were higher for N remaining compared to C

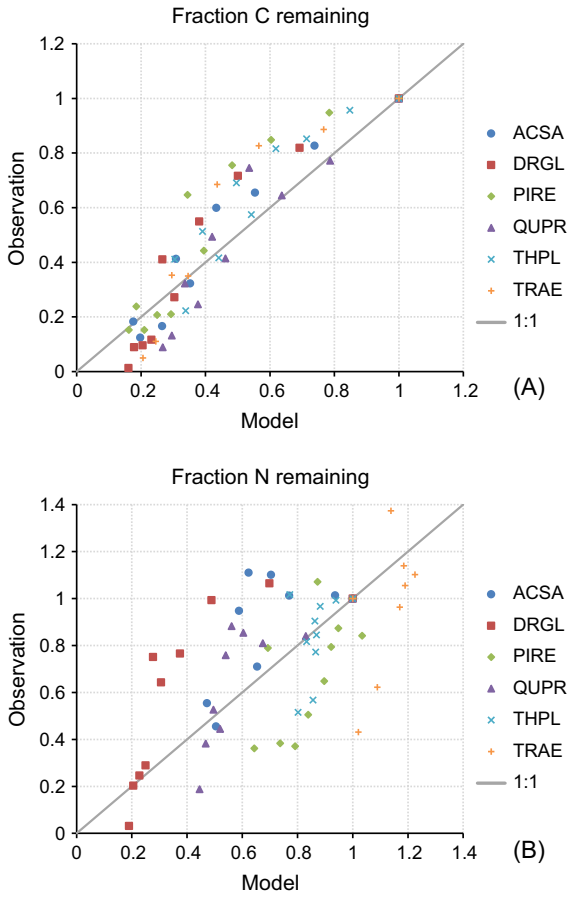

Fig. 3. 1:1 scatterplots of annual remaining C (A) and N (B) fraction between DayCent-UV and LIDET observation at six leaf litter species at Colorado (CPER) site.

remaining (RMSE = 0.16 for N vs. 0.12 for C). DayCent-UV tended to underestimate the fraction of N remaining for DRGL and ACSA and overestimate the fraction of N remaining for PIRE and TRAE (Figs. 2 and 3). DayCent-UV was unable to predict some of the observed species differences in the N remaining; however, there was no overall bias in modeled remaining N fraction.

We used DayCent-UV (optimized using the CPER site data) to simulate C and N remaining data for SEV and JRN sites as an independent validation test. For SEV and JRN, the model was driven with site-specific parameters, such as site's location, soil profile, solar radiation, and weather data, which were adjusted to reflect the environment at the testing sites. Comparison of DayCent-UV results vs. observed C and N remaining for the different plant species at SEV and JRN sites (Fig. 4) showed that the model did a good job simulating the litter C remaining for the different species (RMSE [across-species two-site average C] = 0.12). These results were similar to the modeled C remaining vs. the observed data at CPER site (parameterization/calibration site) (RMSE[CPER] = 0.12) and showed the same bias with an overestimation of C loss for observed C remaining values >0.5 and an underestimation of C loss for observed C remaining <0.3. The results for N remaining had much higher RMSE compared to the C remaining data (across-species two-site average RMSE = 0.21 for N vs. 0.12 for C) consistent with the observed pattern for CPER site. The RMSE of DayCent-UV

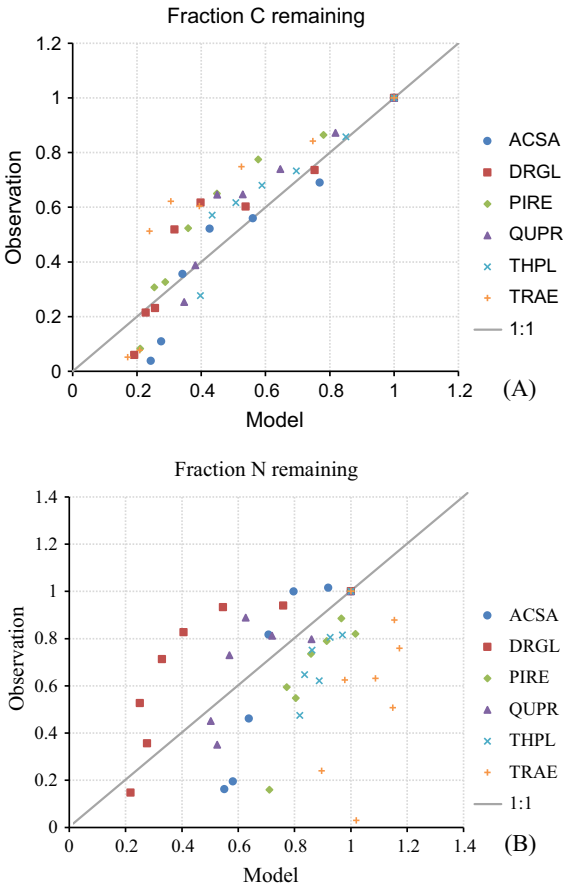

Fig. 4. 1:1 scatterplots of averaged annual remaining C (A) and N (B) fraction between DayCent-UV and LIDET observation at six leaf litter species for (Sevilleta [SEV] and Jornada [JRN]) sites.

Table 3. The maxphoto values as well as the corresponding RMSE values of remaining C and N fractions for the six litter species at Colorado (CPER) site obtained by optimizing individual species (three subcolumns under column DayCent-UV optimized on individual species) and by optimizing across species (three subcolumns under column DayCent-UV optimized across species) using DayCent-UV.

	DayCent-UV optimized on individual species			DayCent-UV optimized across species		
Species	Maxphoto (μg C/kJ [UV_{soil}])	RMSE (remaining C fraction)	RMSE (remaining N fraction)	Maxphoto (μg C/kJ [UV_{soil}])	RMSE (remaining C fraction)	RMSE (remaining N fraction)
ACSA	5.756	0.095	0.272	15.721	0.095	0.274
DRGL	16.241	0.145	0.338	21.862	0.137	0.318
PIRE	14.898	0.174	0.230	11.629	0.164	0.257
QUPR	10.630	0.114	0.120	6.264	0.119	0.186
THPL	0.000	0.116	0.167	2.351	0.129	0.166
TRAE	19.086	0.170	0.279	15.303	0.165	0.316

for C and N at the parameterization and verification sites was similar (RMSE for C: 0.12 [SEV] and 0.12 [JRN]; RMSE for N: 0.04 [SEV] and 0.21 [JRN]). The results also showed that the model consistently overestimated N release for DRGL and underestimated N release for PIRE, THPL, and TRAE species. Both the calibration and validation data sets showed that when all of the litter species were considered, the model was not biased; however, the model did not accurately simulate some of the observed species-specific difference in N release.

Because lignin and cellulose are together in one pool in DayCent-UV, we account for the effects of lignin on photodegradation by imposing a linear relationship between plant initial litter lignin content and the maximum photodecay parameter (maxphoto). The linear equation we use to represent the impact of lignin is shown in the online material (Appendix S2). Analysis of the results showed that the impact of radiation on photodecay decreased with increasing lignin content of the litter. Including the impact of lignin content on photodecay increased the fit of DayCent-UV to the observed C release data (RMSE for remaining C decreased from 0.16 without the lignin impact to 0.12 using the lignin content equation, data not shown). When comparing the maxphoto values for six litter species optimized individually and optimized across species, they were significantly different on some species (i.e., ACSA and QUPR), but the RMSEs for the across-species optimization were not significantly increased (see Table 3) even though the number of parameters being adjusted was greatly reduced (i.e., from 6 to 2).

Effects of photodecay module on spatial and temporal C and N patterns at three LIDET sites

DayCent-UV matched the LIDET observations better than DayCent-Photosyn for both C and N in most time periods and had much higher N loss compared to DayCent-Photosyn. While the observations showed a linear decrease in C for the first 6 years of the experiment and greatly reduced decomposition rates in the last 4 years, both DayCent versions released C with exponential patterns (Fig. 5). Compared with DayCent-Photosyn, DayCent-UV showed slightly slower C decomposition rate in the early stage but showed over 10% more C loss in the later stage. The observations showed balanced N mineralization and immobilization in the first 2 years and net N release in the remaining years. DayCent-UV showed a persistent net N release in the entire 10-year period with the final N remaining fraction at around 0.55, while DayCent-Photosyn showed slight net N immobilization in most time periods except for in the first 2 years, in which period net N release was simulated.

Species averaged C and N remaining vs. time for LIDET observations for CPER, SEV, and JRN sites (Fig. 6) showed that observed C remaining points at three sites were less variable than N remaining; DayCent-UV captured this pattern. However, the observations had a more linear pattern of C remaining vs. time in the first 6 years than DayCent-UV, which predicted an exponential C pattern across the entire period. Both observations and model results showed linear pattern of N remaining vs. time. The model predicted faster than observed C decomposition rates in the

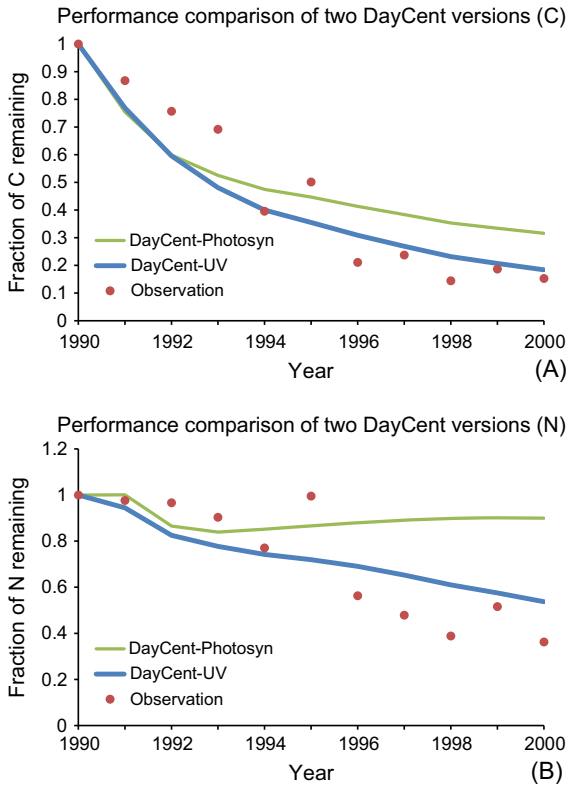

Fig. 5. The across-species average of the remaining C fraction (A) and remaining N fraction (B) at Colorado (CPER) site from LIDET observations and two DayCent versions with (DayCent-UV) and without (DayCent-Photosyn) the photodecay module.

first 3 years than is shown by the observations, but fit the observation points well for both C and N in the later years (Fig. 6). DayCent-UV showed small but distinguishable differences at three sites for both C and N remaining over time with the highest C and N loss at JRN site. The annual solar radiation at CPER site (462.63 W/m^2) was lower than both at SEV site (520.59 W/m^2) and at JRN site (526.10 W/m^2). CPER site generally had the lowest C decomposition rate followed by SEV and JRN sites, although the observed data points were noisy and somewhat intertwined. N release was also the slowest for CPER site. DayCent-UV manifested the same pattern as observations for both C and N after 3–4 years. But at the early stage (i.e., the first 3–4 years), the model showed more variable C and N decomposition rates between sites.

Ecological impacts of photodegradation

Photodecay directly changed the C and N dynamics in surface pools. These changes may indirectly influence other ecosystem processes. To present the ecological impacts of photodegradation, the 90-year (1900–1989) average of the modeled ecological variables were calculated for CPER model runs with (i.e., DayCent-UV) and without (i.e., DayCent-Photosyn) the photodecay module (Table 4). Including the photodecay module caused increases in aboveground and belowground plant production, surface litter net N mineralization, and litter N, but soil organic C and N, soil net N mineralization, and surface litter C all decreased (Table 4). The model results also showed minimal differences (less than 1%) in biotic decomposition rates, and trace gas fluxes (data not shown). The biggest impact of including photodecay were increases in surface litter N mineralization rates by 25%, and surface litter N pools (8%). The decreases in organic soil C and N were a result of the decreased amount of surface litter transferred below ground (greater losses of surface litter and standing dead to the atmosphere due to photodecay). The simulated large increases in surface litter N mineralization were consistent with the observed LIDET litter N release pattern and DayCent-UV simulation results in Fig. 5B.

Discussion

Generally, DayCent-UV fitted the major observed patterns of soil water content in the top 20-cm, aboveground live biomass, and AET well (R^2 values between 0.44 and 0.50; Appendix S7: Fig. S1). However, model results did not fit well with observed NEE (R^2 = 0.23). If we align modeled and observed NEE with precipitation data in the growing season, it is seen that the model underestimated some CO_2 pulses (negative NEE) after big rain events. The mechanisms (Ma et al. 2012, Moyano et al. 2013) behind these respiration pulses (or "Birch Effect") include the following: (1) re-hydrating of dormant microbes; (2) death of microbial biomass and releases of intracellular osmolytes accumulated during the dry period; (3) breaking down of soil microaggregates, which exposes the protected organic matter; (4) microbial cell lysis, which releases

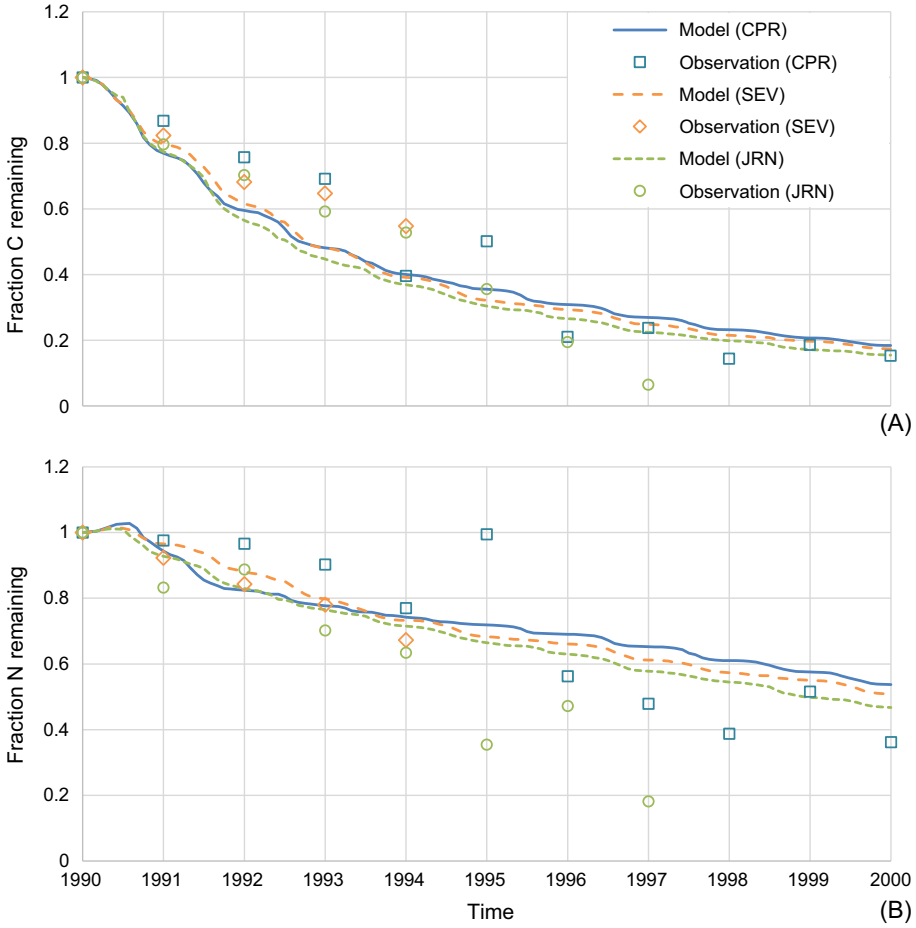

Fig. 6. The across-species averages of the remaining C fraction (A) and remaining N fraction (B) at three LIDET sites (Colorado [CPER], Sevilleta [SEV], and Jornada [JRN]) from DayCent-UV simulations (lines) and LIDET experiment observation (symbols).

cytoplasmic solutes, and uncouples enzymatic activity from cellular respiration; and (5) releasing rapidly decomposable molecules made available via photodegradation and/or extracellular enzymes decomposition accumulated during dry periods. DayCent-UV assumes that soil carbon decay rates are increased (three time normal values) following rainfall events in order to represent the pulse rainfall effect on heterotrophic respiration, yet the model underestimated CO_2 pulses following rainfall events. This suggests that the model needs to include a new fast labile pool that decomposes rapidly following the rainfall events since the size of the CO_2 pulses is similar for each rainfall event during the growing season independent of the time since rainfall (Parton et al. 2012). Alternatively, this may indicate that photodegradation transfers recalcitrant C to the labile pool even during dormant dry periods as suggested in field studies (Ma et al. 2012, Yanni et al. 2015).

Generally, DayCent-UV fitted the observed remaining C vs. time pattern well for both individual species and across-species averages (Figs. 2, 5A, and 6A). Since the model were only run at three sites with similar dry environment conditions, a comprehensive evaluation of model performance should be performed in more diverse environments in the future. DayCent-UV overestimated the C release in the first three years but showed good matches with the observed data during the last four years of the LIDET experiment. In the middle stage (i.e., 4–6 yr), DayCent-UV had lower C decomposition rates and showed

Table 4. Average ecological variables (related to plant productivity, N mineralization, and surface and soil C and N pools) from a 90-year simulation at CPER without and with photodecay (i.e., DayCent-Photosyn and DayCent-UV, respectively).

Ecological variables	DayCent-Photosyn	DayCent-UV	Difference (%)†
Plant productivity (above ground) (g C·m^{-2}·yr^{-1})	48.73	49.29	+1.14
Plant productivity (below ground) (g C·m^{-2}·yr^{-1})	51.04	51.79	+1.47
Surface net N mineralization (g N·m^{-2}·yr^{-1})	0.67	0.84	+25.03
Soil net N mineralization (g N·m^{-2}·yr^{-1})	3.66	3.55	−2.84
Surface litter C pools (g C/m^2)	113.98	95.47	−16.24
Surface litter N pools (g N/m^2)	3.09	3.32	+7.41
Surface biological decay rate (yr^{-1})	0.22	0.22	+0.20
Soil C pools (g C/m^2)	1093.05	1039.35	−4.91
Soil N pools (g N/m^2)	64.33	61.31	−4.70

† Difference (%) = (DayCent-UV − DayCent-Photosyn)/DayCent-Photosyn × 100%.

a more exponential pattern for remaining C than the observed linear pattern in the LIDET data. DayCent-UV only considers instant photodegradation, and the amount of C released is proportional to the solar UV radiation intensity and size of the litter structural pool (for correcting the amount of solar UV radiation intercepted by litter). As a result, materials are photodegraded faster in the earlier stage and slower in the middle and later stages in model results. The discrepancy between model and observation suggests that a cumulative effect of solar UV radiation exposure should be considered in the early and middle stages. A cumulative effect, which means that the impact of UV on mass loss increases over time, has been suggested by other studies. For example, Foereid et al. (2010) concluded that the increasing litter degradability is a more important mechanism for photodegradation than direct light-induced mass loss. King et al. (2012) further concluded that the significance of this facilitation effect heavily depends on length of exposure. Day et al. (2015) showed that photodegradation increased its impact on decomposition as litter aged.

Compared to remaining C results, DayCent-UV showed larger discrepancy for remaining N, but it was able to predict the observed general pattern of N release with time (Fig. 5—averaged over species N release at CPER). The model performance on simulating individual species' N pattern was worse (Figs. 3B and 4B). Some species such as PIRE and TRAE released N slower than observations, while some species such as DRGL released N faster than observations in the entire experiment. In DayCent-UV, the relative C/N ratios between source and target pools and mineral N pools determine N flows between litter pools (Appendix S1). It is possible that the model parameters that control how much N is immobilized or mineralized are not optimal for some species. Since mdr and mti influence the microbial pool size and the N flow is generally tie to the C flow in DayCent-UV (Appendix S1), DayCent-UV has already indirectly incorporated the UV inhibition effects on microbial N immobilization (Smith et al. 2010, Lin and King 2014, Lin et al. 2015*b*, Wang et al. 2015) and the UV facilitation effects by providing more microbial decomposable N compounds (Foereid et al. 2010). The only direct change for N in litter pools is when photodegradation releases C as CO_2 from surface structural, and the associated N flows into surface metabolic. The poorer performance on remaining N vs. time for individual species indicates that DayCent-UV does have the mechanisms to represent species-specific litter N dynamics in arid environments. Observed litter N release data are much more variable than model results (Fig. 2 shows large temporal changes in N release). There have been studies exploring some other potential mechanisms for N in high solar (UV) radiation environment. Some study has suggested that C-use efficiency may be reduced to allow net N release (Zhao et al. 2014). Others have suggested that direct N photodissolution or photodegradation may occur (Mayer et al. 2012).

DayCent-UV matched the observed C remaining slightly better than DayCent-Photosyn in the early stage (i.e., 1–3 yr) but matched much better in the latter stage (i.e., 5–10 yr) (Fig. 5A). Even

though the two models showed similar performance in the early stage, the mechanisms and the C distribution among the four surface litter pools are quite different. DayCent-UV reduced surface structural C with CO_2 loss and added C from surface structural into surface metabolic. The UV inhibition effect (mdr) reduces the surface active (microbes) pool by reducing the consumption of surface metabolic litter. The UV increases the turnover between surface active and slow pools (via mti) and subsequent CO_2 loss. As a result, we saw that DayCent-UV had a significantly larger surface metabolic pool but significantly smaller surface active and slightly smaller surface structural and slow pools than DayCent-Photosyn (data not presented). Additionally, the cumulative CO_2 loss from surface slow and the continuous photodegradation of surface structural caused lower surface litter C remaining in DayCent-UV.

The performance of DayCent-UV on N remaining was much better than that of DayCent-Photosyn especially in the later stage (Fig. 5B). The final remaining N fractions from DayCent-Photosyn, DayCent-UV, and observation were approximately 0.90, 0.55, and 0.45, respectively. Parton et al. (2007) showed that N release from UV impacted dry sites had much faster N release compared to all of the other ecosystems. DayCent-UV generally simulated the persistent net N release found in the observations due to the photodegradation-induced N flow from surface structural to surface metabolic that reduced the intensity of N immobilization from extraneous sources.

The observed negative relationship between the initial lignin fraction of litter (Table 2, column 6) and the individually optimized photodecay rate (Table 3, column 2, maxphoto) suggests that lignin is not the chemical compound that is susceptible to UV degradation. Bontti et al. (2009) also found the strong negative relationships between initial lignin content vs. mass loss and suggested that lignin does not enhance photodegradation. Some field studies did not observe increased lignin loss (Lin and King 2014) or did not find change in lignin (Brandt et al. 2007) under UV exposure. The photodegradation flows in DayCent-UV are imposed on standing dead and surface structural pools, which contain both lignin and cellulose. Therefore, we speculate that cellulose is the major chemical compound susceptible to UV degradation. Some studies reported that degradation of cellulose and/or hemicellulose is responsible for litter mass loss under UV exposure (Rozema et al. 1997, Brandt et al. 2007, 2010). Alternatively, we speculate that photodegradation breaks down encrusting lignin and exposes protected cellulose for biological decomposition (Henry et al. 2008, Austin and Ballaré 2010, Brandt et al. 2010, Frouz et al. 2011). Talbot et al. (2011) found that chemical protection due to the cross-linking between lignins and polysaccharides allowed lignin to control the total decay rates. Lin et al. (2015*a*) used the two-dimensional nuclear magnetic resonance (2D NMR) method to analyze the litter exposed in the field for up to 1 year and found that UV exposure significantly decreased the litter hemicellulose fraction by causing partial degradation (i.e., some lignin structural units and linkages were reduced), not necessarily complete breakdown, of lignin structures.

DayCent-UV equilibrium model runs for Colorado (CPER) site were used to evaluate the ecosystem impact of photodegradation. Photodegradation (in DayCent-UV) increased aboveground and belowground plant production, surface net N mineralization, and surface litter N pool, but decreased surface litter C, soil net N mineralization, and organic soil C and N (see Table 4). Photodegradation of standing dead and surface structural promoted direct C loss from the two pools, enhanced the cellulose accessibility to microbial decomposition, and increased the amount of labile material entering the surface metabolic pool. The decline in organic soil C and N and surface litter C is because more surface C was lost as CO_2 and less C and N were mixed from surface litter into the soil. Photodegradation greatly increased N mineralization from surface structural to surface metabolic supporting experimental studies (Lin et al. 2015*b*, Wang et al. 2015). Photodegradation also increased the total surface N pool because N stayed in the litter as a result of photodecay. This also increased the net N mineralization from the surface pools because microbes need less extraneous mineral N to decompose high C/N ratio materials. Soil net N mineralization decreased because of the reduced input of C and N from surface litter layer into the mineral soil layer. However, the large increase in surface net N mineralization (+25%) more than compensated for the slight reduction (−2.84%) in

soil N mineralization, and the total soil and surface net N mineralization slightly increased.

Conclusions

The calibrated DayCent-UV model fitted the major observed patterns of soil water content in the top 20 cm of soil, aboveground live biomass, and AET (R^2 between 0.44 and 0.50) at CPER but missed some CO_2 spikes after heavy rain events in the observed NEE (R^2 = 0.23). DayCent-UV better fitted the observed LIDET C and N loss patterns than DayCent-Photosyn especially in the later stage. DayCent-UV fitted the observed remaining C vs. time pattern well for both individual species and across-species averages at three (semi-)arid LIDET sites and predicted the observed pattern of N release with time. However, larger discrepancy for remaining N vs. time than for remaining C vs. time for individual species suggests that some mechanisms of photodegradation on N dynamics may be missing. The slight overestimation of C release in the early stage (i.e., years 1–3) and the underestimation in the later stage suggest that the cumulative effect of solar UV radiation exposure should be considered. The negative relationship between litter's initial lignin fraction and the individually optimized photodecay rate suggests that cellulose rather than lignin may be the chemical compound that is responsible for UV degradation. The DayCent-UV equilibrium model runs showed that UV decomposition increased aboveground and belowground plant production, surface net N mineralization, and surface litter N pool, but decreased surface litter C, soil net N mineralization, and organic soil C and N.

Acknowledgments

This research was supported by the USDA NIFA projects 2014-34263-22038, 2015-34263-24070, and 2016-34263-25763. This paper is from a thesis submitted to the Academic Faculty of Colorado State University in partial fulfillment of the requirements for the degree of doctor of philosophy.

Literature Cited

Adair, E. C., W. J. Parton, S. J. Del Grosso, W. L. Silver, M. E. Harmon, S. A. Hall, I. C. Burke, and S. C. Hart. 2008. Simple three-pool model accurately describes patterns of long-term litter decomposition in diverse climates. Global Change Biology 14:2636–2660.

Almagro, M., F. T. Maestre, J. Martínez-López, E. Valencia, and A. Rey. 2015. Climate change may reduce litter decomposition while enhancing the contribution of photodegradation in dry perennial Mediterranean grasslands. Soil Biology and Biochemistry 90:214–223.

Anderson, G. P., A. Berk, P. K. Acharya, L. S. Bernstein, S. M. Adler-Golden, J. Lee, and L. Muratov. 2009. Reformulated atmospheric band model method for modeling atmospheric propagation at arbitrarily fine spectral resolution and expanded capabilities. U.S. Patent, 7593835.

Andrady, A. L., H. Hamid, and A. Torikai. 2011. Effects of solar UV and climate change on materials. Photochemical & Photobiological Sciences 10:292–300.

Austin, A. T. 2011. Has water limited our imagination for aridland biogeochemistry? Trends in Ecology and Evolution 26:229–235.

Austin, A., and C. Ballaré. 2010. Dual role of lignin in plant litter decomposition in terrestrial ecosystems. Proceedings of the National Academy of Sciences of the United States of America 107: 4618–4622.

Austin, A. T., M. S. Méndez, and C. L. Ballaré. 2016. Photodegradation alleviates the lignin bottleneck for carbon turnover in terrestrial ecosystems. Proceedings of the National Academy of Sciences of the United States of America 113:4392–4397.

Austin, A. T., and L. Vivanco. 2006. Plant litter decomposition in a semi-arid ecosystem controlled by photodegradation. Nature 442:555–558.

Baker, N. R., and S. D. Allison. 2015. Ultraviolet photodegradation facilitates microbial litter decomposition in a Mediterranean climate. Ecology 96: 1994–2003.

Berg, B., et al. 1993. Litter mass loss rates in pine forests of Europe and Eastern United States: some relationships with climate and litter quality. Biogeochemistry 20:127–159.

Berk, A., et al. 2006. MODTRAN5: 2006 update. Pages 62331F-1–62331F-8 *in* S. S. Shen and P. E. Lewis, editors. Proceedings of SPIE 6233, Algorithms and Technologies for Multispectral, Hyperspectral, and Ultraspectral Imagery XII, Orlando, Florida, USA.

Bond-Lamberty, B., and A. M. Thomson. 2010. Temperature-associated increases in the global soil respiration record. Nature 464:579–582.

Bontti, E. E., J. P. Decant, S. M. Munson, M. A. Gathany, A. Przeszlowska, M. L. Haddix, S. Owens, I. C. Burke, W. J. Parton, and M. E. Harmon. 2009. Litter

decomposition in grasslands of Central North America (US Great Plains). Global Change Biology 15:1356–1363.

Brandt, L. A., C. Bohnet, and J. Y. King. 2009. Photochemically induced carbon dioxide production as a mechanism for carbon loss from plant litter in arid ecosystems. Journal of Geophysical Research 114: G02004.

Brandt, L. A., J. Y. King, S. E. Hobbie, D. G. Milchunas, and R. L. Sinsabaugh. 2010. The role of photodegradation in surface litter decomposition across a grassland ecosystem precipitation gradient. Ecosystems 13:765–781.

Brandt, L. A., J. Y. King, and D. G. Milchunas. 2007. Effects of ultraviolet radiation on litter decomposition depend on precipitation and litter chemistry in a shortgrass steppe ecosystem. Global Change Biology 13:2193–2205.

Braswell, B. H., W. J. Sacks, E. Linder, and D. S. Schimel. 2005. Estimating diurnal to annual ecosystem parameters by synthesis of a carbon flux model with eddy covariance net ecosystem exchange observations. Global Change Biology 11:335–355.

Bristow, K. L., and G. S. Campbell. 1984. On the relationship between incoming solar radiation and daily maximum and minimum temperature. Agricultural and Forest Meteorology 31:159–166.

Caldwell, M. M., L. O. Björn, J. F. Bornman, S. D. Flint, G. Kulandaivelu, A. H. Teramura, and M. Tevini. 1998. Effects of increased solar ultraviolet radiation on terrestrial ecosystems. Journal of Photochemistry and Photobiology B: Biology 46:40–52.

Ciais, P., et al. 2013. Carbon and other biogeochemical cycles. Pages 465–570 *in* T. F. Stocker, D. Qin, G.-K. Plattner, M. Tignor, S. K. Allen, J. Boschung, A. Nauels, Y. Xia, V. Bex, and P. M. Midgley, editors. Climate change 2013: the physical science basis. Contribution of Working Group I to the Fifth Assessment Report of the Intergovernmental Panel on Climate Change. Cambridge University Press, Cambridge, UK and New York, New York, USA.

Conn, A. R., N. I. M. Gould, and Ph L Toint. 2000. Trust-region methods. SIAM/MPS Series on Optimization. Society for Industrial and Applied Mathematics, Philadelphia, Pennsylvania, USA.

Cory, R. M., K. McNeill, J. P. Cotner, A. Amado, J. M. Purcell, and A. G. Marshall. 2010. Singlet oxygen in the coupled photochemical and biochemical oxidation of dissolved organic matter. Environmental Science & Technology 44:3683–3689.

Cramer, W., D. W. Kicklighter, A. Bondeau, B. Moore III, G. Churkina, B. Nemry, A. Ruimy, A. L. Schloss, and The Participants of the Potsdam NPP Model Intercomparison. 1999. Comparing global models of terrestrial net primary productivity (NPP): overview and key results. Global Change Biology 5:1–15.

Day, T. A., R. Guenon, and C. T. Ruhland. 2015. Photodegradation of plant litter in the Sonoran Desert varies by litter type and age. Soil Biology & Biochemistry 89:109–122.

Day, T. A., E. T. Zhang, and C. T. Ruhland. 2007. Exposure to solar UV-B radiation accelerates mass and lignin loss of *Larrea tridentata* litter in the Sonoran Desert. Plant Ecology 193:185–194.

Del Grosso, S. J., A. D. Halvorson, and W. J. Parton. 2008. Testing DAYCENT model simulations of corn yields and nitrous oxide emissions in irrigated tillage systems in Colorado. Journal of Environmental Quality 37:1383–1389.

Del Grosso, S. J., A. R. Mosier, W. J. Parton, and D. S. Ojima. 2005. DAYCENT model analysis of past and contemporary soil N_2O and net greenhouse gas flux for major crops in the USA. Soil and Tillage Research 83:9–24.

Del Grosso, S. J., W. J. Parton, C. A. Keough, and M. Reyes-Fox. 2011. Special features of the DayCent modeling package and additional procedures for parameterization, calibration, validation, and applications. Pages 155–176 *in* L. R. Ahuja and L. Ma, editors. Methods of introducing system models into agricultural research. American Society of Agronomy, Madison, Wisconsin, USA.

Del Grosso, S. J., W. J. Parton, A. R. Mosier, M. D. Hartman, J. Brenner, D. S. Ojima, D. S. Schimel. 2001. Simulated interaction of carbon dynamics and nitrogen trace gas fluxes using the DAYCENT model. Pages 303–332 *in* S. Hansen, M. J. Shaffer, and L. Ma, editors. Modeling carbon and nitrogen dynamics for soil management. CRC Press, Boca Raton, Florida, USA.

Del Grosso, S. J., W. J. Parton, A. R. Mosier, D. S. Ojima, A. E. Kulmala, and S. Phongpan. 2000. General model for N_2O and N_2 gas emissions from soils due to dentrification. Global Biogeochemical Cycles 14:1045–1060.

Dirks, I., Y. Navon, D. Kanas, R. Dumbur, and J. M. Grünzweig. 2010. Atmospheric water vapor as driver of litter decomposition in Mediterranean shrubland and grassland during rainless seasons. Global Change Biology 16:2799–2812.

Escobedo, J. F., E. N. Gomes, A. P. Oliveira, and J. Soares. 2010. Ratios of UV, PAR and NIR components to global solar radiation measured at Botucatu site in Brazil. Renewable Energy 36: 169–178.

Feng, X., K. M. Hills, A. J. Simpson, J. K. Whalen, and M. J. Simpson. 2011. The role of biodegradation and photo-oxidation in the transformation of

terrigenous organic matter. Organic Geochemistry 42:262–274.

Fernández Zenoff, V., F. Siñeriz, and M. E. Farías. 2006. Diverse responses to UV-B radiation and repair mechanisms of bacteria isolated from high-altitude aquatic environments. Applied and Environmental Microbiology 72:7857–7863.

Foereid, B., J. Bellarby, W. Meier-Augenstein, and H. Kemp. 2010. Does light exposure make plant litter more degradable? Plant and Soil 333:275–285.

Foereid, B., M. J. Rivero, O. Primo, and I. Ortiz. 2011. Modelling photodegradation in the global carbon cycle. Soil Biology & Biochemistry 43:1383–1386.

Frouz, J., T. Cajthaml, and O. Mudrak. 2011. The effect of lignin photodegradation on decomposability of *Calamagrostis epigeios* grass litter. Biodegradation 22:1247–1254.

Gallo, M. E., A. Porras-Alfaro, K. J. Odenbach, and R. L. Sinsabaugh. 2009. Photoacceleration of plant litter decomposition in an arid environment. Soil Biology & Biochemistry 41:1433–1441.

Gallo, M. E., R. L. Sinsabaugh, and S. E. Cabaniss. 2006. The role of ultraviolet radiation in litter decomposition in arid ecosystems. Applied Soil Ecology 34:82–91.

Gehrke, C., U. Johanson, T. V. Callaghan, D. Chadwick, and C. H. Robinson. 1995. The impact of enhanced ultraviolet-B radiation on litter quality and decomposition processes in Vaccinium leaves from the Subarctic. Oikos 72:213–222.

George, B., E. Suttie, A. Merlin, and X. Deglise. 2005. Photodegradation and photostabilisation of wood – the state of the art. Polymer Degradation and Stability 88:268–274.

Gholz, H. L., D. A. Wedin, S. M. Smitherman, M. E. Harmon, and W. J. Parton. 2000. Long-term dynamics of pine and hardwood litter in contrasting environments: toward a global model of decomposition. Global Change Biology 6:751–765.

Harmon, M. 2013. LTER Intersite Fine Litter Decomposition Experiment (LIDET), 1990 to 2002. Long-Term Ecological Research. Forest Science Data Bank, Corvallis, Oregon, USA. http://andrewsforest.oregonstate.edu/data/abstract.cfm?dbcode=TD023

Harmon, M. E., B. Bond-Lamberty, J. Tang, and R. Vargas. 2011. Heterotrophic respiration in disturbed forests: a review with examples from North America. Journal of Geophysical Research 116: G00K04.

Heisler-White, J. L., A. K. Knapp, and E. F. Kelly. 2008. Increasing precipitation event size increases aboveground net primary productivity in a semi-arid grassland. Oecologia 158:129–140.

Henry, H. A. L., K. Brizgys, and C. B. Field. 2008. Litter decomposition in a California annual grassland: interactions between photodegradation and litter layer thickness. Ecosystems 11:545–554.

Hughes, K. A., B. Lawley, and K. K. Newsham. 2003. Solar UV-B radiation inhibits the growth of Antarctic terrestrial fungi. Applied and Environmental Microbiology 69:1488–1491.

Hutchinson, K. J., K. L. King, G. R. Nicol, and D. R. Wilkinson. 1990. Methods for evaluating the role of residues in the nutrient cycling economy of pastures. Pages 291–314 *in* A. F. Harrison, P. Ineson, and O. W. Heal, editors. Nutrient cycling in terrestrial ecosystems, field methods, application and interpretation. Elsevier Applied Science, Amsterdam, The Netherlands.

Irmak, S., E. Istanbulluoglu, and A. Irmak. 2008. An evaluation of evapotranspiration model complexity against performance in comparison with Bowen ratio energy balance measurements. Transactions of the ASABE 51:1295–1310.

Jornada Basin LTER. 2012. LTER Weather Station daily summary climate data. Jornada Basin LTER, Long Term Ecological Research Network. http://dx.doi.org/10.6073/pasta/abf2b27152d632ab2ab27c6c71a8a10a

Kielbassa, C., L. Roza, and B. Epe. 1997. Wavelength dependence of oxidative DNA damage induced by UV and visible light. Carcinogenesis 18:811–816.

King, J. Y., L. A. Brandt, and E. C. Adair. 2012. Shedding light on plant litter decomposition: advances, implications and new directions in understanding the role of photodegradation. Biogeochemistry 111:57–81.

Kurbanyan, K., K. L. Nguyen, P. To, E. V. Rivas, A. M. Lueras, C. Kosinski, M. Streryo, A. Gonzales, D. A. Mah, and E. D. Stemp. 2003. DNA-protein cross-linking via guanine oxidation: dependence upon protein and photosensitizer. Biochemistry 42: 10269–10281.

Kurz-Besson, C., M.-M. Coûteaux, J. M. Thiéry, B. Berg, and J. Remacle. 2005. A comparison of litterbag and direct observation methods of Scots pine needle decomposition measurement. Soil Biology and Biochemistry 37:2315–2318.

Laguna, M., and R. Martí. 2003. Scatter search: methodology and implementations in C. Kluwer Academic Publishers, Boston, Massachusetts, USA.

Lauenroth, W. K. 2013. SGS-LTER Standard Production Data: 1983-2008 Annual Aboveground Net Primary Production on the Central Plains Experimental Range, Nunn, Colorado, USA 1983–2008, ARS Study Number 6. http://hdl.handle.net/10217/81141

Lee, H., T. Rahn, and H. Throop. 2012. An accounting of C-based trace gas release during abiotic plant litter degradation. Global Change Biology 18: 1185–1195.

Lin, Y., and J. Y. King. 2014. Effects of UV exposure and litter position on decomposition in a California grassland. Ecosystems 17:158–168.

Lin, Y., J. Y. King, S. D. Karlen, and J. Ralph. 2015*a*. Using 2D NMR spectroscopy to assess effects of UV radiation on cell wall chemistry during litter decomposition. Biogeochemistry 125:427–436.

Lin, Y., R. D. Scarlett, and J. Y. King. 2015*b*. Effects of UV photodegradation on subsequent microbial decomposition of *Bromus diandrus* litter. Plant and Soil 395:263–271.

Liu, S., R. Hu, G. Cai, S. Lin, J. Zhao, and Y. Li. 2014. The role of UV-B radiation and precipitation on straw decomposition and topsoil C turnover. Soil Biology & Biochemistry 77:197–202.

Lloyd, J., and J. A. Taylor. 1994. On the temperature dependence of soil respiration. Functional Ecology 8:315–323.

Long-Term Intersite Decomposition Experiment Team (LIDET). 1995. Meeting the challenge of long-term, broad-scale ecological experiments. Publication No. 19. LTER Network Office, Seattle, Washington, USA.

Ma, S. Y., D. D. Baldocchi, J. A. Hatala, M. Detto, and J. C. Yuste. 2012. Are rain-induced ecosystem respiration pulses enhanced by legacies of antecedent photodegradation in semi-arid environments? Agricultural and Forest Meteorology 154:203–213.

Mayer, L. M., K. R. Thornton, L. L. Schick, J. D. Jastrow, and J. W. Harden. 2012. Photodissolution of soil organic matter. Geoderma 170:314–321.

Meentemeyer, V. 1978. Macroclimate and lignin control of litter decomposition rates. Ecology 59:465–472.

Melillo, J. M., J. D. Aber, and J. F. Muratore. 1982. Nitrogen and lignin control of hardwood leaf litter decomposition dynamics. Ecology 63:621–626.

Messenger, D. J., A. R. McLeod, and S. C. Fry. 2009. The role of ultraviolet radiation, photosensitizers, reactive oxygen species and ester groups in mechanisms of methane formation from pectin. Plant, Cell & Environment 32:1–9.

Mitchell, D. L., and D. Karentz. 1993. The induction and repair of DNA photodamage in the environment. Pages 345–377 *in* A. R. Young, editor. Environmental UV photobiology. Plenum Press, New York, New York, USA.

Moody, S. A., et al. 2001. The direct effects of UV-B radiation on *Betula pubescens* litter decomposing at four European field sites. Plant Ecology 154:27–36.

Moore, D. I. 2014. Meteorology Data at the Sevilleta National Wildlife Refuge, New Mexico (1987-). Long Term Ecological Research Network. http://dx.doi.org/10.6073/pasta/669823a9c848c979d2888912a56678c3

Moorhead, D. L., and T. Callaghan. 1994. Effects of increasing ultraviolet B radiation on decomposition and soil organic matter dynamics: a synthesis and modelling study. Biology and Fertility of Soils 18:19–26.

Moorhead, D. L., W. S. Currie, E. B. Rastetter, W. J. Parton, and M. E. Harmon. 1999. Climate and litter quality controls on decomposition: an analysis of modeling approaches. Global Biogeochemical Cycles 13:575–589.

Moyano, F. E., S. Manzoni, and C. Chenu. 2013. Responses of soil heterotrophic respiration to moisture availability: an exploration of processes and models. Soil Biology & Biochemistry 59:72–85.

National Centers for Environmental Information, NOAA. 2015. Climate data online. http://www.ncdc.noaa.gov/cdo-web/

National Water and Climate Center, NRCS, USDA. 2015. Colorado SCAN Site Nunn #1 (2017) daily weather data. http://www.wcc.nrcs.usda.gov/nwcc/site?site num=2017

Nemani, R. R., C. D. Keeling, H. Hashimoto, W. M. Jolly, S. C. Piper, C. J. Tucker, R. B. Myneni, and S. W. Running. 2003. Climate-driven increases in global terrestrial net primary production from 1982 to 1999. Science 300:1560–1563.

Olson, J. S. 1963. Energy storage and the balance of producers and decomposers in ecological systems. Ecology 44:322–331.

Pancotto, V. A., O. E. Sala, M. Cabello, N. I. López, T. M. Robson, C. L. Ballaré, M. M. Caldwell, and A. L. Scopel. 2003. Solar UV-B decreases decomposition in herbaceous plant litter in Tierra del Fuego, Argentina: potential role of an altered decomposer community. Global Change Biology 9:1465–1474.

Pancotto, V. A., O. E. Sala, T. M. Robson, M. M. Caldwell, and A. L. Scopel. 2005. Direct and indirect effects of solar ultraviolet-B radiation on long-term decomposition. Global Change Biology 11:1982–1989.

Parton, W. J. 2013. SGS-LTER Standard Met Data: 1969-2010 Manually Collected Aboveground and Belowground Meteorological Data collected on the Central Plains Experimental Range, Nunn, Colorado, USA, ARS Study Number 4. http://hdl.handle.net/10217/82446

Parton, W. J., M. Hartman, D. Ojima, and D. Schimel. 1998. DAYCENT and its land surface submodel: description and testing. Global and Planetary Change 19:35–48.

Parton, W. J., E. A. Holland, S. J. Del Grosso, M. D. Hartman, R. E. Martin, A. R. Mosier, D. S. Ojima, and D. S. Schimel. 2001. Generalized model for NO_x and N_2O emissions from soils. Journal of Geophysical Research 106:17403–17419.

Parton, W., J. Morgan, D. Smith, S. Del Grosso, L. Prihodko, D. Lecain, R. Kelly, and S. Lutz. 2012. Impact of precipitation dynamics on net ecosystem productivity. Global Change Biology 18:915–927.

Parton, W. J., D. S. Schimel, C. V. Cole, and D. S. Ojima. 1987. Analysis of factors controlling soil organic levels of grasslands in the Great Plains. Soil Science Society of America Journal 51:1173–1179.

Parton, W. J., R. J. Scholes, K. Day, J. O. Carter, and R. Kelly. 2011. CENTURY-SAVANNA model for tree-grass ecosystems. Pages 443–446 *in* M. J. Hill and N. P. Hanan, editors. Ecosystem function in Savannas: measurement and modeling at landscape to global scale. CRC Press, Boca Raton, Florida, USA.

Parton, W. J., J. W. B. Stewart, and C. V. Cole. 1988. Dynamics of C, N, P and S in grassland soils – a model. Biogeochemistry 5:109–131.

Parton, W., et al. 2007. Global-scale similarities in nitrogen release patterns during long-term decomposition. Science 315:361–364.

Pérez-Harguindeguy, N., S. Díaz, J. H. C. Cornelissen, F. Vendramini, M. Cabido, and A. Castellanos. 2000. Chemistry and toughness predict leaf litter decomposition rates over a wide spectrum of functional types and taxa in central Argentina. Plant and Soil 218:21–30.

Peters, D. P. C., et al. 2013. Long-term trends in ecological systems: a basis for understanding responses to global change. Technical Bulletin Number 1931. U.S. Department of Agriculture, Agricultural Research Service, Jornada Experimental Range, Las Cruces, New Mexico, USA.

Physical Sciences Division, ESRL, NOAA. 2015. NCEP Reanalysis data (NARR), NOAA/OAR/ESRL PSD, Boulder, Colorado, USA. http://www.esrl.noaa.gov/psd/

Rangeland Resources Research Unit, ARS. 2015. CPER weather data. http://www.ars.usda.gov/Main/docs.htm?docid=11120

Rozema, J., M. Tosserams, H. Nelissen, L. van Heerwaarden, R. A. Broekman, and N. Flierman. 1997. Stratospheric ozone reduction and ecosystem processes: Enhanced UV-B radiation affects chemical quality and decomposition of leaves of the dune grassland species *Calamagrostis epigeios*. Plant Ecology 128:285–294.

Rutledge, S., D. I. Campbell, D. Baldocchi, and L. A. Schipper. 2010. Photodegradation leads to increased carbon dioxide losses from terrestrial organic matter. Global Change Biology 16:3065–3074.

Savage, K. E., W. J. Parton, E. A. Davidson, S. E. Trumbore, and S. D. Frey. 2013. Long-term changes in forest carbon under temperature and nitrogen amendments in a temperate northern hardwood forest. Global Change Biology 19:2389–2400.

Smith, W. K., W. Gao, H. Steltzer, M. D. Wallenstein, and R. Tree. 2010. Moisture availability influences the effect of ultraviolet-B radiation on leaf litter decomposition. Global Change Biology 16:484–495.

Song, X., C. Peng, H. Jiang, Q. Zhu, and W. Wang. 2013. Direct and indirect effects of UV-B exposure on litter decomposition: a meta-analysis. PLoS ONE 8:e68858.

Stehfest, E., M. Heistermann, J. A. Priess, D. S. Ojima, and J. Alcamo. 2007. Simulation of global crop production with the ecosystem model DayCent. Ecological Modelling 209:203–219.

Straube, J. R. 2011. Integration of variable photosynthetic capacity into a biogeochemical model. Thesis. Colorado State University, Fort Collins, Colorado, USA.

Talbot, J. M., D. J. Yelle, J. Nowick, and K. K. Treseder. 2011. Litter decay rates are determined by lignin chemistry. Biogeochemistry 108:279–295.

Thornton, P. E., and S. W. Running. 1999. An improved algorithm for estimating incident daily solar radiation from measurements of temperature, humidity, and precipitation. Agricultural and Forest Meteorology 93:211–228.

Trofymow, J. A., C. M. Preston, and C. E. Prescott. 1995. Litter quality and its potential effect on decay rates of materials from Canadian forests. Water, Air, and Soil Pollution 82:215–226.

Ugray, Z., L. Lasdon, J. Plummer, F. Glover, J. Kelly, and R. Martí. 2007. Scatter search and local NLP solvers: a multistart framework for global optimization. INFORMS Journal on Computing 19:328–340.

Vähätalo, A., M. Søndergaard, L. Schlüter, and S. Markager. 1998. Impact of solar radiation on the decomposition of detrital leaves of eelgrass *Zostera marina*. Marine Ecology Progress Series 170:107–117.

Virzo De Santo, A., B. Berg, F. A. Rutigliano, A. Alfani, and A. Fioretto. 1993. Factors regulating early-stage decomposition of needle litters in five different coniferous forests. Soil Biology & Biochemistry 25:1423–1433.

Wang, J., L. Liu, X. Wang, and Y. Chen. 2015. The interaction between abiotic photodegradation and microbial decomposition under ultraviolet radiation. Global Change Biology 21:2095–2104.

Whitford, W. G., V. Meentemeyer, T. R. Seastedt, K. Cromack Jr., D. A. Crossley Jr., P. Santos, R. L. Todd, and J. B. Waide. 1981. Exceptions to the AET model: deserts and clear-cut forest. Ecology 62:275–277.

Yanni, S. F., E. C. Suddick, and J. Six. 2015. Photodegradation effects on CO_2 emissions from litter and SOM and photo-facilitation of microbial decomposition in a California grassland. Soil Biology & Biochemistry 91:40–49.

Zepp, R. G., T. V. Callaghan, and D. J. Erickson. 1998. Effects of enhanced solar ultraviolet radiation on biogeochemical cycles. Journal of Photochemistry and Photobiology B: Biology 46:69–82.

Zhao, H., G. Huang, J. Ma, Y. Li, and L. Tang. 2014. Decomposition of aboveground and root litter for three desert herbs: mass loss and dynamics of mineral nutrients. Biology and Fertility of Soils 50:745–753.

Supporting Information

Additional Supporting Information may be found online at: http://onlinelibrary.wiley.com/doi/10.1002/ecs2.1631/full